International Journal of Mass Spectrometry 280 (2009) 149–153

Contents lists available at ScienceDirect

International Journal of Mass Spectrometry

journal homepage: www.elsevier.com/locate/ijms

Long-lived metastable anions of hydrogen halides

M. Čížek*, Jiří Horáček

Charles University Prague, Faculty of Mathematics and Physics, Institute of Theoretical Physics, V Holešovičkách 2, 180 00 Praha 8, Czech Republic

ARTICLE INFO

Article history:
Received 9 June 2008
Received in revised form 29 July 2008
Accepted 31 July 2008
Available online 8 August 2008

The paper is dedicated to 75th birthday of Zdeněk Herman.

PACS:
34.15.Ry
52.20.Fs
52.20.Hv

Keywords:
Molecular anion
Resonance
Electron–molecule collision
Ion–atom collision

ABSTRACT

We search for narrow resonances in cross-sections for electron collisions with HCl, DCl, HBr and DBr molecules, calculated with the nonlocal resonance model. Narrow resonances corresponding to long-lived metastable states of anionic molecules are indeed found in both elastic and vibrational excitation cross-sections. The largest lifetime $\tau = 0.11$ ms is predicted for HBr^- with rotational quantum number $J = 20$. For HCl we find maximum $\tau = 0.6$ ns for $J = 22$ and $\tau = 0.6$ μs for $J = 33$ in DCl. A surprising isotope effect is found for DBr, where the largest lifetime is $\tau = 1.5$ μs, i.e., much smaller than for HBr.

1. Introduction

The smallest molecular anion H_2^- is unstable, but can temporarily be formed in both $e^- + H_2$ [1] and $H + H^-$ [2] collisions at low energies. Typical lifetimes are of the order of a few femtoseconds. In 1998, we predicted the existence of resonances with lifetimes of the order of picoseconds in the associative detachment cross-section [3]. Later, we studied these resonances in detail, discovering a group of metastable states of H_2^-, which are stabilised against autodetachment by rotation [4,5]. Their lifetime can exceed microseconds. These ions were also unambiguously identified experimentally [4] in products of sputtering of hydrogen rich compounds with energetic Cs^+ ions. The lifetime of the most stable states of H_2^-, HD^- and D_2^- was measured in a storage ring [6] in agreement with the uncertainty limits given by the theory [5].

The large lifetime of the resonances can be understood from the shape of the adiabatic potential energy curve of the ground state of the anion [4]. This potential energy function, which is purely attractive for nonrotating molecules $J = 0$, develops, for larger J, a barrier which suppresses the flux to the inner region of small internuclear distances, where the autodetachment of the electron occurs. Although the autodetachment dynamics itself is not correctly described by adiabatic potential function, the energy of the resonances can be, to a good approximation, determined as the energy of a bound state in the outer potential energy well.

In [7], we furthermore studied ocillatory structures (often called boomerang oscillations) in the cross-section for vibrational excitation of H_2 and some other diatomic molecules by electron impact. It turns out that there is a smooth transition between the oscillatory structures and the above mentioned narrow resonances in the cross-section. While the boomerang oscillations can be related to the changes in the phase of the wave function as a function of collision energy, the narrow resonances are accompanied by an increase of the wave function's amplitude in the energy-independent (stationary state) description. In [7] we also show that while this distinction can be made for some cases, there is often a transition region (considering changes in energy or angular momentum) where the structures are caused by a combination of the two effects. The boomerang oscillations are present in number of other systems. They are known to exist in cross-sections for vibrational excitation of HCl by electron impact [8,9] as well as in HBr [10], HF [11] and some larger molecules [12]. It is therefore a natural question if the long-lived narrow resonances stabilised by rotation also exist in these systems.

* Corresponding author. Tel.: +420 221912513; fax: +420 21912496.
E-mail address: Martin.Cizek@mff.cuni.cz (M. Čížek).

1387-3806/$ – see front matter © 2008 Elsevier B.V. All rights reserved.
doi:10.1016/j.ijms.2008.07.034

Low-energy electron collisions with hydrogen halides exhibit rich resonance effects and threshold phenomena (see, for example, [13] for a review of both experimental and theoretical results for HCl and HBr). The shape of the adiabatic potentials of both HCl^- and HBr^- exhibits an outer potential-energy well. A narrow resonance with the width in the milli-electronvolt range have previously been observed in the experimental vibrational excitation cross-section [8]. The decay of the possible metastable states of HX^- through autodetachment into the $HX(J,v)+e^-$ channel is a process which is closely related to the associative detachment (AD) reaction

$$H + X^- \rightarrow HX(J, v) + e^-.$$

In the autodetachment process, the initial condition is given by the state trapped in the outer well in the Born–Oppenheimer potential for HX^- (for large R, where the local complex potential approximation is justified), while in the AD, the initial condition is given by the incoming wave in the same potential. It is know from previous calculations and experiments [14,15,16] that the cross-sections for associative detachment exhibit clear Wigner cusps at the energies where the detachment into $HX(J,v)+e^-$ is closed for some rovibrational state (J,v). The cusps can be observed both in energy and J dependencies. We can therefore expect to observe unusual effects in the dependence of the resonance parameters for the possible $HX(J,v)+e^-$ metastable states on the rotational energy of the molecule. These effect would also be a clear manifestation of the violation of the local complex potential approximation in the anion decay, since the Wigner cusps appear only as a consequence of the energy dependence of the nonlocal potential [14].

In this paper, we systematically search for narrow resonances in calculated cross-sections for $e^- + HX$ and $X^- + H$ collisions for X = F, Cl and Br. We also find the parameters (energy and lifetime) of the resonances and we study the transition between the boomerang oscillations and the narrow resonances for these systems. The paper is organised as follows: in the next section we refer shortly to the theoretical description and the models for the studied systems. We also discuss in some detail the relation of the structures in the cross-sections to the shape of the potential energy curves and describe the localisation of resonances and the determination of their parameters. The last section summarises and compares the results in all systems.

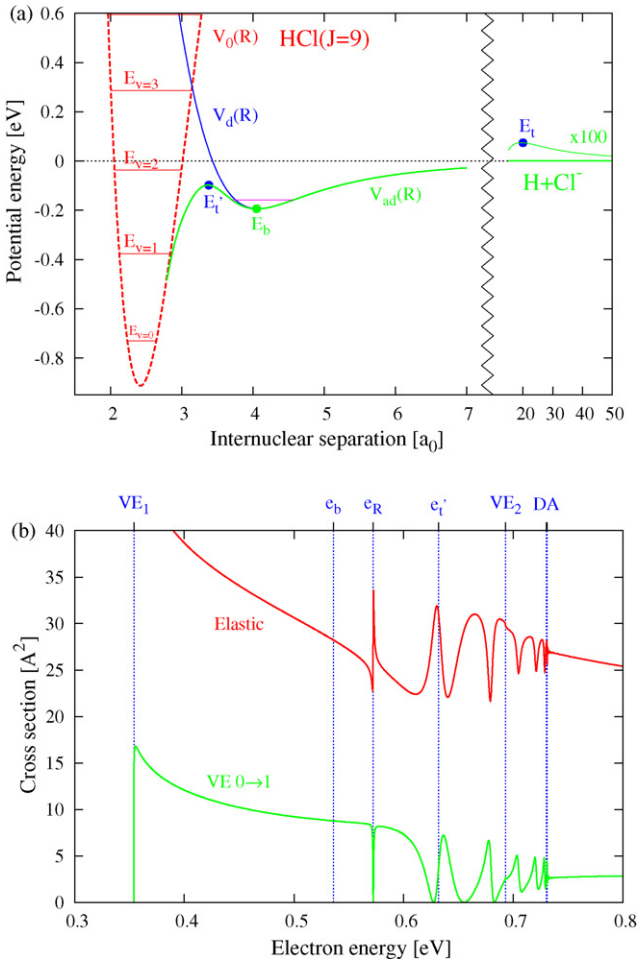

Fig. 1. Potential energy curves for the nonlocal resonance model for $HCl(v,J)+e^-$ for the rotational state $J=8$ (a). The energies relevant for the interpretation of the elastic electron scattering and the vibrational excitation cross-sections (b) are also marked in (a).

2. Calculation of the cross-sections and location of resonances

In [10,11,17] we studied the processes of vibrational excitation (VE), dissociative attachment (DA) and associative detachment (AD)

$$e^- + HX(v) \rightarrow e^- + HX(v'), \quad (1)$$

$$e^- + HX(v) \rightarrow H + X^-, \quad (2)$$

$$H + X^- \rightarrow e^- + HX(v), \quad (3)$$

for the hydrogen halides X = F, Cl, Br within the nonlocal resonance model. The cross-sections for these processes have been calculated from the solution of the Lippmann–Schwinger equation for the component of the total wavefunction of the system projected on a diabatic discrete state representing the temporarily formed HX^- state (see the above references for the details of the calculations or [18] for the review of the theory). As an example, we show the basic functions describing the model and the vibrational excitation cross-sections for HCl in Fig. 1. The upper plot shows the relevant potential energy surfaces for the ground electronic state of HCl ($V_0(R)$, dashed line), with vibrational states indicated, the adiabatic ground electronic state of HCl^- ($V_{ad}(R)$) and the discrete state potential ($V_d(R)$, solid lines). While the potential for the discrete state is identical to the adiabatic potential for HCl^- at large internuclear separations R, the two potentials become separated near the crossing with $V_0(R)$. This splitting is controlled by another function $V_{d\varepsilon}(R)$ which characterizes the coupling between the discrete state and the continuum state with electron energy ε (see, for example, [18]). The energy dependence of $V_{d\varepsilon}(R)$ for $\varepsilon \rightarrow 0$ is essential for the behaviour of the scattering quantities near thresholds for electron scattering on the neutral molecule in different vibrational states. This behaviour depends on long range interaction between the molecule and the additional electron [18]. For H_2 molecule there is smooth onset of $V_{d\varepsilon}(R) \sim \varepsilon^{1.5}$ resulting from the p-wave character of the electron scattering dictated by symmetry. This smoothness somewhat suppresses the threshold effects. On the other hand, in hydrogen halides this behaviour has sharp onset as ε^α with $\alpha < 0.5$ due to the nonzero dipole moment of the molecules. This is an important difference, since the function $V_{d\varepsilon}(R)$ controls the autodetachment process.

The adiabatic potential energy curve for the HCl^- ion has a remarkable shape, exhibiting a barrier which separates the outer ($R > 3.5a_0$) and the inner ($R > 3.5a_0$) regions. The outer potential well can support quasibound states as also indicated in Fig. 1. Depending on their location, these states can be seen in the cross-sections for various processes as shown in Fig. 1(b). The graph shows the energy dependence of the cross-section for vibrational excitation

from the ground state to the first vibrationally excited state, and the cross-section for the elastic $e^- + HCl$ scattering [17].

The shape of the potentials in Fig. 1 depends also on the rotational state of the molecule. The functions are plotted for the angular momentum $J = 8$. With increasing J, all the curves (and the vibrational levels E_ν) are shifted upward due to the centrifugal term $J(J+1)/2\mu R^2$. This term is strongest at short distances, which means that the top of the inner barrier $E_{t'}$ moves up faster than the bottom of the well E_b, making the autodetachment of the quasibound states more difficult for higher J. On the other hand, as the bottom of the potential well moves up, at $J = 23$, $E_b > 0$, and all resonances can decay outwards by dissociation to $H + Cl^-$. This decay is suppressed, however, by tunnelling through the outer barrier E_t. This barrier is very low for $J = 8$ (note that a different scale is used for the tail of the potentials in Fig.1), but increases for higher J.

The position of the structures in the cross-section in the lower part of the figure can be understood from the energy levels in the upper part. The threshold for vibrational excitation is $E_{VE1} = E_1 - E_0$. Similarly, the energies of the barriers and the resonance relative to the ground vibrational state, $e_b = E_b - E_0$, $e_r = E_R - E_0$, $e_t = E_t - E_0$, $e_{t'} = E_{t'} - E_0$, and the thresholds for higher excitation, $E_{VE2} = E_2 - E_0$, and dissociative attachment, $E_{DA} = -E_0$, are marked on the electron energy axis of the cross-section plot. Narrow resonances can be located only above the bottom of the outer potential well e_b and significantly below the top of both barriers e_t,$e_{t'}$. There is only one such narrow resonance in Fig. 1, marked as e_R. Above $e_{t'}$, the resonances evolve smoothly into boomerang oscillations as discussed in [7]. The boomerang oscillations are terminated at the energy e_t (indistinguishable from the DA threshold in the plot for $J = 8$). It is interesting to note the effect of the second VE threshold on the cross-sections. The threshold is visible as a small cusp in the cross-sections and also the amplitude of the oscillations decreases at this energy.

Once we understand the location of the resonances as quasibound states in the outer well of $V_l(R)$, we can calculate the cross-section in this region on a very fine energy grid. According to the well-known Fano formula [19], the cross-section near a resonance is proportional to

$$\frac{(q+\varepsilon)^2}{1+\varepsilon^2}, \quad \text{with } \varepsilon = \frac{E - E_R}{\Gamma/2}, \tag{4}$$

where E_R is the energy and Γ is the width of the resonance. The later is related to the lifetime of the metastable resonance state through the relation $\tau = \hbar/\Gamma$.

3. Results and discussion

In the previous section, we discussed how narrow resonances in the elastic electron scattering and vibrational excitation cross-sections of HCl can be localised and how the lifetime of the associated quasibound states can be found. The results for the HCl molecule are summarised in Fig. 2; the figure shows the J-dependence of the potential energy minima (E_b) and maxima (E_t, $E_{t'}$). The positions of the narrow resonances are shown for each J as dots, with the size of the dot indicating the inverse width of the resonance (so that the states with large lifetime are better visible). As discussed above, all narrow resonances must be located between E_b and min(E_t,$E_{t'}$). In the region between E_t and $E_{t'}$, the resonances evolve into boomerang oscillations. To elucidate the transition of the boomerang oscillations into narrow resonances, we also show the positions of the local minima and local maxima of the elastic electron scattering cross-section. The region between E_t and $E_{t'}$ is filled with these extrema. As J increases, the extrema cross $E_{t'}(J)$. One maximum and one minimum always get close to each other,

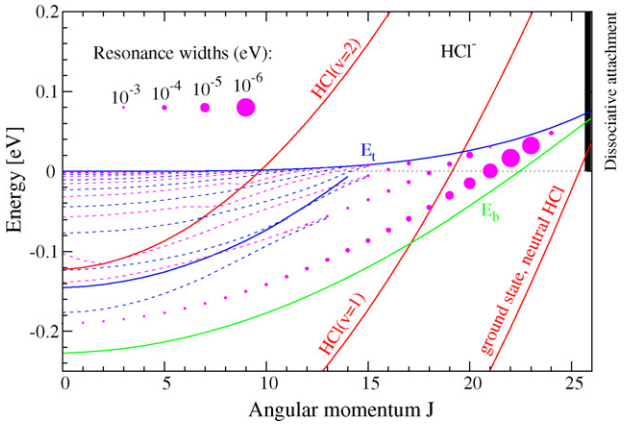

Fig. 2. Summary of metastable states in HCl^-. The dependence of the resonance energy on the rotational state of the molecule is shown (circles). The resonance lifetime is indicated by the size of the dot. The thresholds (red lines) for the decay into $HCl(v) + e^-$ are indicated for different vibrational states v; the threshold for the $H + Cl^-$ decay channel corresponds to zero energy as indicated on the right edge of the figure. The energies of the local maxima (blue lines) and minima (green line) in the effective potential of the anion are also shown. The dashed lines show the extrema of the cross-section (see text). (For interpretation of the references to color in this figure legend, the reader is referred to the web version of the article.)

which is a signature of the formation of a narrow resonance. For $J = 15$, there exists a maximum of four narrow resonance states with widths between 0.1 and 1 meV. For smaller J's, some of them transform into boomerang oscillations. For larger J's, they are pushed above E_t, disappearing in the smooth continuum. To understand the lifetimes of the resonances, we also plot rovibrational energies $E_\nu(J)$ of the neutral molecule $HCl(\nu,J)$ for $\nu = 0, 1, 2$ in the same figure. Note that majority of the resonances can decay into both $e^- + HCl$ ($\nu = 0$) and $e^- + HCl$ ($\nu = 1$), but for J around 20, the channel $e^- + HCl$ ($\nu = 1$) is closed. This has a stabilising effect on the resonances and the lifetimes increase significantly.

The widths Γ and energies E_R of the quasibound states of HCl^- are collected in Fig. 3. The progression of the resonances corresponding to the ground vibrational state in the outer potential well are marked by $\nu = 0$ and connected with dotted line, similarly as the excited states by $\nu = 1$, 2, 3. To distinguish the rotational quantum numbers, some J's are marked with a different shape of the dot. We see the stabilising effect of the rotation as the width of each resonance decreases with increasing J, until the resonance energy

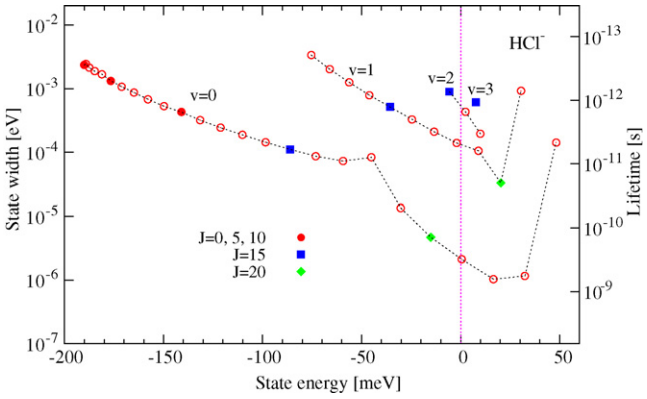

Fig. 3. Resonance width/lifetime versus energy for HCl. The rotational quantum number is indicated by type of the dot. States with the same number of nodes v in the outer potential well are connected by the dotted lines. The threshold for the dissociation into $H + Cl^-$ is marked by a vertical dotted line.

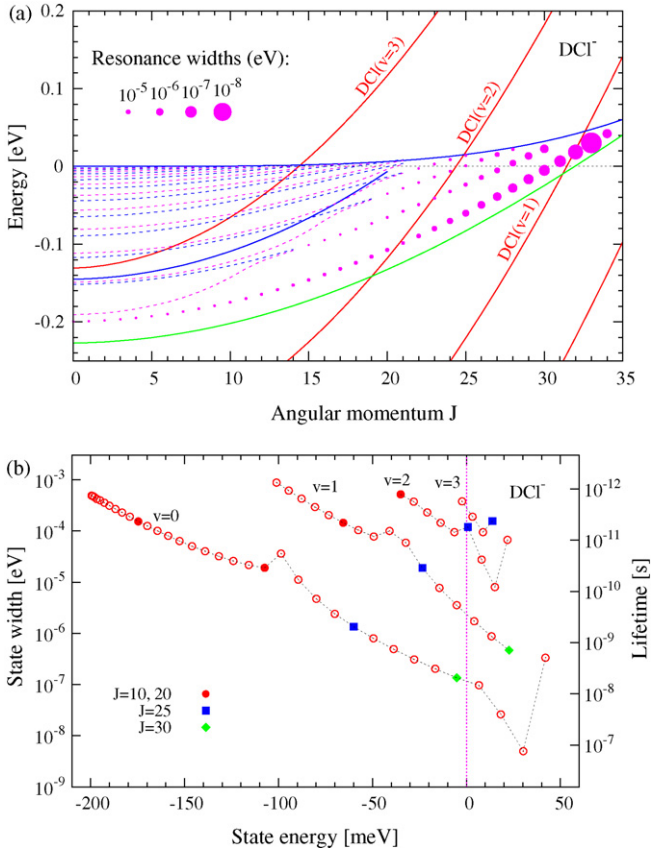

Fig. 4. Summary of metastable states in DCl^- (a) depicted as in Fig. 2 for HCl and plot of the resonance width (lifetime) versus its energy (b).

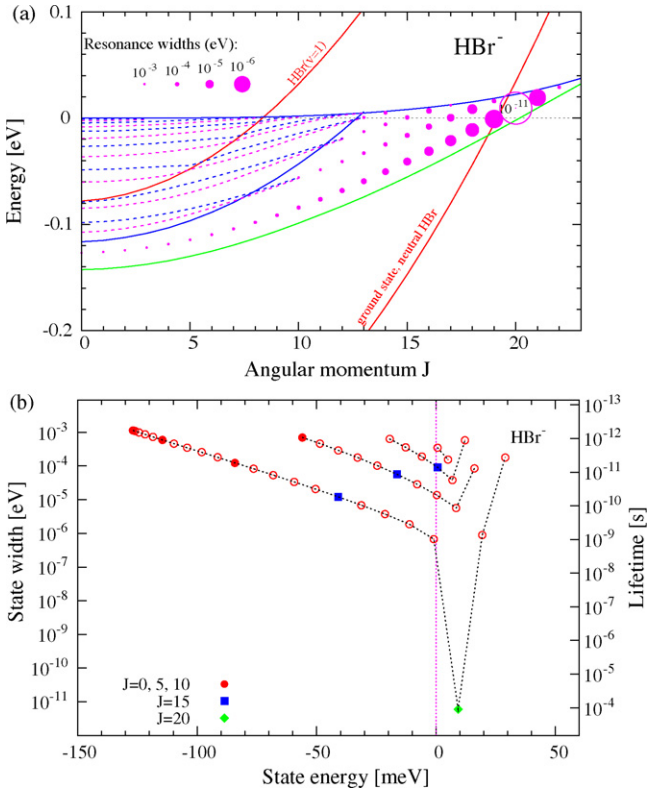

Fig. 5. Summary of the metastable states of HBr^- (a), depicted as in Fig. 2 for HCl, and the plot of the resonance width (lifetime) versus its energy (b).

is finally pushed above $E_R = 0$, where the resonance can decay to $H + Cl^-$ and the width increases again as the energy $E_R(J)$ approaches $E_t(J)$. It is noteworthy that this trend is interrupted by the closing of the $e^- + HCl$ ($v = 1$) channel leading to $\Gamma(J = 18) > (J = 17)$. This effect is closely related to the Wigner cusps predicted [14] and observed [15,16] in electron energy spectra resulting from associative detachment in $H + Cl^-$ collisions.

In our calculation, we can easily study also the isotope effect. The potential energy curves remain the same for DCl^-, only the reduced mass is approximately doubled. The centrifugal term $J(J+1)/2\mu R^2$ in the potential energy is thus half of that for HCl^-. As a consequence, the overall picture in Fig. 4 is similar to Fig. 2 for HCl, but the rotational quantum numbers J are in general factor of $\sqrt{2}$ larger. The width of the resonances is mainly controlled by tunnelling. It is thus not surprising that the resonances get narrower for the heavier system. The narrowest resonance attains a lifetime of a fraction of a microsecond, which may allow direct detection by mass spectrometry. The energy-versus-width plot (in the lower part of the figure) shows similar features as for HCl. In particular, Wigner cusps can be observed for $v = 0$ at $J = 21$, 31 and at $J = 23$, 25 for $v = 1$, 2, respectively.

Another hydrogen halide anion which we studied previously in connection with electron–molecule scattering [10] and ion–atom scattering was HBr^-. We have performed the same analysis as for HCl^-. The potential energy curves are of similar shape (see Fig. 1 in [13]) and narrow resonances in the cross-sections can be found in the energy interval determined by the local extrema of the adiabatic HBr^- potential energy curve. The results are summarised in energy-versus-angular-momentum and width-versus-energy plots in Fig. 5. The main difference compared to HCl^- is the position of the final states $HBr(v)$ relative to the $H + Br^-$ resonances. There is only one decay channel, $HBr(v) + e^-$, available for almost all resonances and even this channel closes at $J = 20$. The only remaining decay channel for the resonances with $J > 19$ becomes $H + Br^-$, which is accessible by tunnelling through the outer barrier. This barrier is rather low but extends to large R. The lifetime of the narrowest resonance thus reaches $\tau \sim 0.1$ ms for $J = 20$. It is important to mention, however, that this lifetime is exponentially sensitive to small changes in the potential energy curve as was previously observed for some resonances in H_2^- [5]. The value can thus be considered only as an order-of-magnitude estimate, but it is highly probable that the state is experimentally observable. Wigner cusps are less pronounced in this system, since they appear in the region where the lifetime changes rapidly due to the opening of the dissociative channel ($H + Br^-$). It is also interesting to mention that the narrowest resonances cannot be seen in the $e^- + HBr$ scattering cross-section, because they are located below the threshold. We therefore searched for these resonances in the elastic $H + Br^-$ cross-section, which can also be calculated within the nonlocal resonance model. During the calculation of the energy dependence of the cross-section, we also monitor the magnitude of the wave function $|\psi(R_b)|^2$ at the position of the bottom of the outer potential well. This helps us to find the narrow resonances, since $|\psi(R_b)|^2$ steadily grows reaching a maximum at resonance, unlike the cross-section, which is determined by the background scattering, and only close to resonance energy (at distance comparable to the width of the resonance) it changes rapidly according to the Fano formula.

The isotope effect for HBr^-/DBr^- is qualitatively similar as for the HCl/DCl system. In general, there are more resonances in DBr^- due to the higher values of J, and the lifetimes are longer. At the same time, the spacing of the final states available for the decay is smaller. Thanks to this, we can see the effect of the closing of

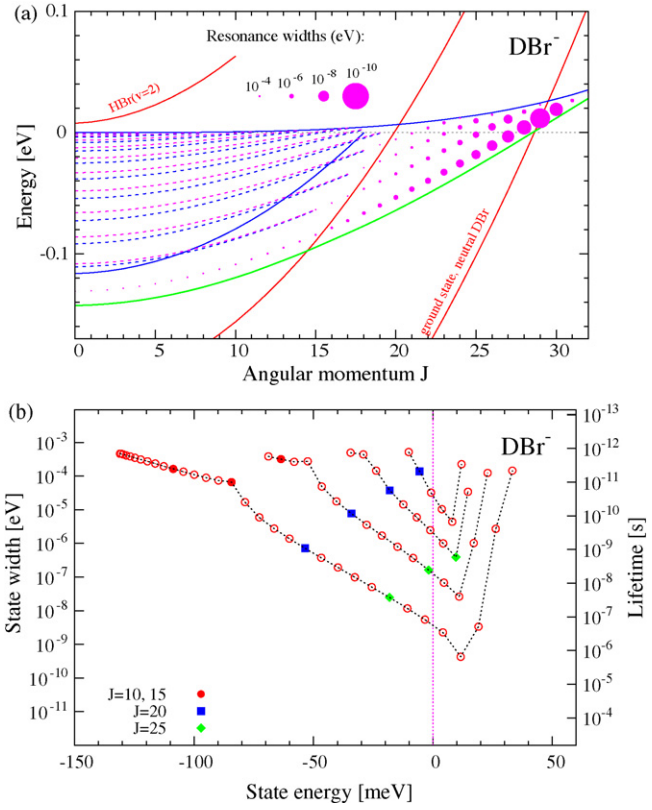

Fig. 6. Summary of the metastable states of DBr^- (a), depicted as in Fig. 2 for HCl, and the plot of the resonance width (lifetime) versus its energy (b).

Table 1
Lifetimes of the most stable anion states and their energies (in units of eV) with respect to the thresholds of the decay channels

Resonance	Lifetime (s)	$e^- + HX$	$H + X^-$
HCl^- ($J=22$)	6.4×10^{-10}	0.2120	0.0166
HCl^- ($J=23$)	5.7×10^{-10}	0.1725	0.0325
DCl^- ($J=32$)	2.5×10^{-8}	0.2378	0.0184
DCl^- ($J=33$)	1.3×10^{-7}	0.2098	0.0302
HBr^- ($J=19$)	9.8×10^{-10}	0.0048	−0.0009
HBr^- ($J=20$)	1.1×10^{-4}	−0.0251	0.0093
HBr^- ($J=21$)	7.4×10^{-10}	−0.0570	0.0194
DBr^- ($J=28$)	2.9×10^{-7}	0.0232	0.0042
DBr^- ($J=29$)	1.5×10^{-6}	0.0011	0.0117
DBr^- ($J=30$)	2.0×10^{-7}	−0.0219	0.0191

Negative energies indicate closed channels.

the $DBr(v=1)$ channel in Fig. 6. Surprisingly, the maximum lifetime found is smaller than that for HBr. This is caused by the sensitivity of the high-J resonances to the value of the energy relative to the top of the outer barrier E_t. Since the J-dependence is discretised, the value of the energy just falls into a less favourable position. Let us emphasise that the value of lifetime of this resonance is extremely sensitive to variations of the potential energy surface. The theoretical prediction is thus not very reliable.

To summarize, the energies and widths of the most important (that is, most long-lived) resonances of HCl^-/DCl^- and HBr^-/DBr^- are given in Table 1.

4. Other hydrogen halides and comparison to H_2

Within the nonlocal resonance model for $e^- + HF$ [11], it turns out that the adiabatic potential of the anion does not develop a significant outer potential well when the rotational quantum number J is increased. The potential just changes from attractive to repulsive. A very shallow well appears for $J = 24 - 27$, but is less that 10 meV deep and therefore does not support any narrow resonances. In the adiabatic potential of HI^- there exists an outer potential well [20] similar as for HCl^- and HBr^- even for $J = 0$. This well is located below ground state of neutral HI. The corresponding states of HI^- are thus bound and can be studied with conventional methods for bound molecular states using the Born–Oppenheimer approximation.

The results for the narrow resonances in HCl^- and HBr^- discussed above, are in many respects quite similar to our previous results for H_2^- [5]. This may be somewhat surprising, since the electron resonance in H_2^- is of p-wave character and, unlike hydrogen halides, the molecule poses no dipole moment. We see the reason for this similarity in the fact that the outer well in the HX^- potential is, in both cases, formed due to attractive polarisation interaction between H and X^- ion and the inner barrier is resulting from the avoided crossing between HX^- potential and the $HX + e^-$ continuum. The nonzero dipole moment has profound effect on the threshold behaviour of cross-sections as discussed in Section 2 and it is also reflected in the presence of Wigner cusps in the J-dependence of the widths in hydrogen halides which are not present in H_2.

Acknowledgements

We thank Wolfgang Domcke for careful reading and improving the text of this paper. This work has been supported by Grant Agency of the Academy of Sciences of the Czech Republic (project GAAV no. IAA100400501) and by "Výzkumný záměr" grant no. MSM0021620860 of MŠMT.

References

[1] J.C.Y. Chen, J.L. Peacher, Phys. Rev. 163 (1967) 103.
[2] J. Mizuno, J.C.Y. Chen, Phys. Rev. 187 (1969) 167.
[3] M. Čížek, J. Horáček, W. Domcke, J. Phys. B 31 (1998) 2571.
[4] R. Golser, H. Gnaser, W. Kutschera, A. Priller, P. Steier, A. Wallner, M. Čížek, J. Horáček, W. Domcke, Phys. Rev. Lett. 94 (2005) 223003.
[5] M. Čížek, J. Horáček, W. Domcke, Phys. Rev. A 75 (2007) 012507.
[6] O. Heber, R. Golser, H. Gnaser, D. Berkovits, Y. Toker, M. Eritt, M.L. Rappaport, D. Zajfman, Phys. Rev. A 73 (2006) 060501.
[7] K. Houfek, M. Čížek, J. Horáček, Chem. Phys. 347 (2008) 250.
[8] M. Allan, M. Čížek, J. Horáček, W. Domcke, J. Phys. B 33 (2000) L209.
[9] W. Vanroose, C.W. McCurdy, T.N. Rescigno, Phys. Rev. A 68 (2003) 052713.
[10] M. Čížek, J. Horáček, A.C. Sergenton, D.B. Popović, M. Allan, W. Domcke, T. Leininger, F.X. Gadea, Phys. Rev. A 63 (2001) 062710.
[11] M. Čížek, J. Horáček, M. Allan, I.I. Fabrikant, W. Domcke, J. Phys. B 36 (2003) 2837.
[12] M. Allan, J. Phys. B 35 (2002) L387.
[13] M. Čížek, J. Horáček, M. Allan, W. Domcke, Czech. J. Phys. 52 (2002) 1057.
[14] M. Čížek, J. Horáček, F.A.U. Thiel, H. Hotop, J. Phys. B 34 (2001) 983.
[15] S. Živanov, M. Allan, M. Čížek, J. Horáček, F.A.U. Thiel, H. Hotop, Phys. Rev. Lett. 89 (2002) 073202.
[16] S. Živanov, M. Čížek, J. Horáček, M. Allan, J. Phys. B 36 (2003) 3513.
[17] M. Čížek, J. Horáček, W. Domcke, Phys. Rev. A 60 (1999) 2873.
[18] W. Domcke, Phys. Rep. 208 (1991) 97.
[19] U. Fano, Phys. Rev. 124 (1961) 1866.
[20] J. Horáček, W. Domcke, H. Nakamura, Z. Phys. D 42 (1997) 181.